J|A|C|S
ARTICLES
Published on Web 04/06/2007

Shell-Cross-Linked Cylindrical Polyisoprene-*b*-Polyferrocenylsilane (PI-*b*-PFS) Block Copolymer Micelles: One-Dimensional (1D) Organometallic Nanocylinders

Xiaosong Wang,[†,§] Kun Liu,[†] André C. Arsenault,[†] David A. Rider,[†] Geoffrey A. Ozin,*[,†] Mitchell A. Winnik,*[,†] and Ian Manners*[,†,‡]

Contribution from the Department of Chemistry, University of Toronto, 80 Saint George Street, Toronto, Ontario, M5S 3H6, Canada and The School of Chemistry, The University of Bristol, Bristol, BS8 1TS, England

Received December 5, 2006; E-mail: gozin@chem.utoronto.ca; mwinnik@chem.utoronto.ca; ian.manners@bristol.ac.uk

Abstract: We report the creation and properties of colloidally stable shell-cross-linked cylindrical organometallic block copolymer micelles with adjustable length and swellability. The one-dimensional (1D) structures with semicrystalline polyferrocenylsilane (PFS) cores and polyisoprene (PI) coronas were initially self-assembled from PI-*b*-PFS block copolymers in a PI-selective solvent such as hexane. The length of the cylinders could be varied from hundreds of nanometers to several tens of micrometers by adjusting solution conditions, using various solvents such as hexane, decane, or hexane/THF (or toluene) mixtures. The cylindrical micelles with vinyl groups in the PI corona were cross-linked through a Pt(0)-catalyzed hydrosilylation reaction using 1,1,3,3-tetramethyl disiloxane as a cross-linker at room temperature. The shell cross-linking significantly increased the stability of the micelles relative to the un-cross-linked precursors as no fragmentation was observed upon sonication in solution. In addition, the structural integrity of the micelles was also enhanced after solvent removal; a solid sample was successfully microtomed and then examined using TEM, which revealed circular cross-sections for the PI-*b*-PFS micelles with an average diameter of ca. 15 nm. We also discovered that shell cross-linking is a prerequisite for generating ceramic replicas through the pyrolysis of PI-*b*-PFS aggregates. Moreover, we were able to pattern the cross-linked micelles on a flat substrate by microfluidic techniques, generating perpendicularly crossed lines of aligned micelles. In short, the shell-cross-linked PI-*b*-PFS 1D organometallic aggregates are a promising new type of nanomaterial with intriguing potential applications.

Introduction

One-dimensional (1D) nano-objects have attracted growing attention due to their unique physical traits, including their electronic, magnetic, optical, and mechanical properties, and potential applications.[1,2] The study of 1D nanostructures is a rapidly expanding interdisciplinary area of research. Nanocylinders can be synthesized by a variety of methods, and one of the most promising involves the self-assembly of block copolymers.[3−6] For example, in a selective solvent, diblock copolymers can self-assemble into micelles, which consist of insoluble blocks as the cores and soluble blocks as the coronas.[7] The exterior and interior properties of the resulting 1D micelles are defined by the functionality of the corresponding polymer blocks. However, the development of their applications in materials science has been hindered by their poor physical stability that arises from the presence of only weak supermolecular interactions binding the aggregates together. For example, in a good solvent for both blocks, the micelles will dissociate into individual unimers.

Over the past decade, several groups have demonstrated that cross-linking the core[8,9] or shell[3,10] of spherical micelles can dramatically improve the colloidal stability of these aggregates. Cross-linked spherical micelles are of considerable interest as nanospheres and nanocages.[11,12] For example, Wooley and coworkers used shell-cross-linked micelles as synthetic analogs of viral capsids for selective uptake and release of small and

† University of Toronto.
‡ The University of Bristol.
§ Current address: Department of Colour and Polymer Chemistry, University of Leeds, Leeds, LS2 9JT, England.

(1) Xia, Y.; Yang, P.; Sun, Y.; Wu, Y.; Mayers, B.; Gates, B.; Yin, Y.; Kim, F.; Yan, H. *Adv. Mater.* **2003**, *15*, 353−389.
(2) Lieber, C. M. *Solid State Commun.* **1998**, *107*, 607−616.
(3) Zhang, Q.; Remsen, E. E.; Wooley, K. L. *J. Am. Chem. Soc.* **2000**, *122*, 3642−3651.
(4) Won, Y. Y.; Davis, H. T.; Bates, F. S. *Science* **1999**, *283*, 960−963.
(5) Law, M.; Sirbuly, D. J.; Johnson, J. C.; Goldberger, J.; Saykally, R. J.; Yang, P. *Science* **2004**, *305*, 1269−1273.
(6) Liu, G.; Qiao, L.; Guo, A. *Macromolecules* **1996**, *29*, 5508−5510.
(7) Hamley, I. W. *The Physics of Block Copolymers*; Oxford University Press, Inc.: New York, 1998.
(8) Guo, A.; Liu, G.; Tao, J. *Macromolecules* **1996**, *29*, 2487−2493.
(9) Tao, J.; Liu, G.; Ding, J.; Yang, M. *Macromolecules* **1997**, *30*, 4084−4089.
(10) Thurmond, K. B.; Kowalewski, T.; Wooley, K. L. *J. Am. Chem. Soc.* **1997**, *119*, 6656−6665.
(11) Wooley, K. L. *Chem. Eur. J.* **1997**, *3*, 1397−1399.
(12) Liu, G. *Curr. Opin. Colloid Interface Sci.* **1998**, *3*, 200−208.

10.1021/ja068730f CCC: $37.00

large guests.[13] Recently, these workers also demonstrated that shell-cross-linked micelles could be used for surface functionalization.[14,15] In addition, Armes et al. used water-soluble cross-linked micelles as pH-responsive particulate emulsifiers.[16] Wooley and Hawker produced fluorescent nanoparticles through a chemical modification of the cores of shell-cross-linked micelles.[17]

Compared to the situation for spherical micelles, shell-cross-linked cylindrical micelles derived from direct block copolymer self-assembly are virtually unexplored.[18−20] Wooley et al. briefly reported that intermediate non-spherical morphologies such as fragmenting rods and pearl-necklace structures could be trapped through shell cross-linking reactions.[19] Stupp et al. reversibly cross-linked peptide−amphiphile nanofibers for mineralization applications.[18] Using a different approach, Liu and co-workers synthesized cross-linked cylindrical assemblies starting from a triblock copolymer in the solid state.[21−23] The triblock copolymer was initially self-assembled into an array of cylinders and cross-linked in bulk. Upon interaction with a good solvent for the polymer, the cross-linked fibers were dispersed into solution, forming discrete nanofibers. The length of the fibers was adjusted by ultrasonic fragmentation. They further converted these cylinders into nanotubes lined with interior carboxylic acid groups by selective core degradation.[22] By a similar process, Müller and co-workers developed a novel type of amphiphilic nanocylinder, known as Janus particles, which have a cross-linked polybutadiene core and a shell containing phase-separated polystyrene and poly(methyl methacrylate) chains.[24]

Hybridizing organic assemblies with inorganic materials is a strategy which allows the introduction of new properties that complement those available with all-organic materials.[25−27] As an example of the use of this approach, Liu and co-workers successfully encapsulated inorganic nanoparticles such as Fe_2O_3 inside polymeric nanotubes, leading to one-dimensional functional nanomaterials. An alternative approach to the introduction of new functionality is to create hybrid nanostructures via the self-assembly of inorganic block copolymers. This approach may offer several advantages over post-hybridization, such as a simplified fabrication scheme and the creation of more well-defined nanostructures.

Polyferrocenylsilanes (PFSs) are an interesting class of metal-containing polymers that are readily accessible by ring-opening polymerization (ROP) routes and possess a range of intriguing properties as a result of the presence of inorganic elements of Fe and Si in the backbone.[28,29] Two features of interest to us are the presence of redox activity as a consequence of the reversible Fe(II)/Fe(III) couple and an ability to act as high-yield pyrolytic precursors to ceramics containing Fe nanoparticles in a C/SiC matrix. These properties are important with respect to the magnetic and catalytic properties and display applications of PFS materials.[30,31]

PFS block copolymers can be synthesized by living ROP. We have previously shown that self-assembly of PFS-containing block copolymers such as PFS-*b*-PDMS (PDMS, polydimethylsiloxane)[32] and PI-*b*-PFS (PI, polyisoprene)[33] in hydrocarbon solvents such as hexane and decane affords cylindrical micelles with a PFS core and a corona of PDMS or PI. The ability of the block copolymers to aggregate into cylindrical nanostructures even when the corona-forming block is much longer than the PFS block has been attributed to the semicrystalline nature of the PFS block that was used.[34,35]

We also successfully used PFS-*b*-PDMS and PFS-*b*-PI nanocylinders as precursors to produce nanoceramic lines via treatment with an oxygen or a hydrogen plasma.[36,37] However, in spite of a range of promising potential applications, many of our attempts to explore these novel cylindrical organometallic nanostructures were impeded by the colloidal and mechanical instability of the aggregates. To tackle this problem, we developed Pt(0)-catalyzed hydrosilylation shell-cross-linking reactions to stabilize PI-*b*-PFS nanocylinders by taking advantage of the vinyl groups present in the PI coronas.[38] This shell-cross-linking approach has been extended to elongated structures formed by self-assembly of PFS-*b*-PMVS (PMVS, polymethylvinylsiloxane)[39] because vinyl groups in PMVS corona are as reactive as those in PI chains. We further demonstrated that cross-linked PFS-*b*-PMVS micelles are robust reactive templates for the synthesis of metal nanoparticles. In a common solvent, cross-linked PFS-*b*-PMVS micelles formed a type of nanogel with solvated PFS chains covered by a PMVS network. The PFS components of the nanogels were found to be able to react with silver ions, leading to encapsulation of silver nanoparticles inside PFS-*b*-PMVS cross-linked aggregates.[40]

(13) Turner, J. L.; Chen, Z.; Wooley, K. L. *J. Controlled Release* **2005**, *109*, 189−202.
(14) Qi, K.; Ma, Q.; Remsen, E. E.; Clark, C. G.; Wooley, K. L. *J. Am. Chem. Soc.* **2004**, *126*, 6599−6607.
(15) Joralemon, M. J.; O'Reilly, R. K.; Hawker, C. J.; Wooley, K. L. *J. Am. Chem. Soc.* **2005**, *127*, 16892−16899.
(16) Fujii, S.; Cai, Y.; Weaver, J. V. M.; Armes, S. P. *J. Am. Chem. Soc.* **2005**, *127*, 7304−7305.
(17) O'Reilly, R. K.; Joralemon, M. J.; Hawker, C. J.; Wooley, K. L. *Chem. Eur. J.* **2006**, *12*, 6776−6786.
(18) Hartgerink, J. D.; Beniash, E.; Stupp, S. I. *Science* **2001**, *294*, 1684−1688.
(19) Ma, Q.; Remsen, E. E.; Clark, C. G.; Kowalewski, T.; Wooley, K. L. *Proc. Natl. Acad. Sci. U.S.A.* **2002**, *99*, 5058−5063.
(20) Yan, X.; Liu, G.; Haeussler, M.; Tang, B. Z. *Chem. Mater.* **2005**, *17*, 6053−6059.
(21) Liu, G. *Adv. Mater.* **1997**, *9*, 437−439.
(22) Stewart, S.; Liu, G. *Angew. Chem., Int. Ed.* **2000**, *39*, 340−344.
(23) Liu, G.; Ding, J.; Qiao, L.; Guo, A.; Dymov, B. P.; Gleeson, J. T.; Hashimoto, T.; Saijo, K. *Chem. Eur. J.* **1999**, *5*, 2740−2749.
(24) (a) Liu, Y.; Abetz, V.; Müller, A. H. E. *Macromolecules* **2003**, *36*, 7894−7898. (b) For work on core−shell cylinders, see: Djalali, R.; Li, S.-Y.; Schmidt, M. *Macromolecules* **2002**; *35*; 4282−4288.
(25) Bockstaller, M. R.; Mickiewicz, R. A.; Thomas, E. L. *Adv. Mater.* **2005**, *17*, 1331−1349.
(26) Braun, E.; Eichen, Y.; Sivan, U.; Ben-Yoseph, G. *Nature* **1998**, *391*, 775−778.
(27) Stupp, S. I.; Braun, P. V. *Science* **1997**, *277*, 1242−1248.
(28) Foucher, D. A.; Tang, B. Z.; Manners, I. *J. Am. Chem. Soc.* **1992**, *114*, 6246−6248.
(29) Manners, I. *Science* **2001**, *294*, 1664−1666.
(30) Lu, J. Q.; Kopley, T. E.; Moll, N.; Roitman, D.; Chamberlin, D.; Fu, Q.; Liu, J.; Russell, T. P.; Rider, D. A.; Manners, I.; Winnik, M. A. *Chem. Mater.* **2005**, *17*, 2227−2231.
(31) (a) Kulbaba, K.; Manners, I. *Macromol. Rapid. Commun.* **2001**, *22*, 711−724. (b) Arsenault, A. C.; Míguez, H.; Kitaev, V.; Ozin, G. A.; Manners, I. *Adv. Mater.* **2003**, *15*, 503−507.
(32) Massey, J.; Power, K. N.; Manners, I.; Winnik, M. A. *J. Am. Chem. Soc.* **1998**, *120*, 9533−9540.
(33) Cao, L.; Manners, I.; Winnik, M. A. *Macromolecules* **2002**, *35*, 8258−8260.
(34) Massey, J. A.; Temple, K.; Cao, L.; Rharbi, Y.; Raez, J.; Winnik, M. A.; Manners, I. *J. Am. Chem. Soc.* **2000**, *122*, 11577−11584.
(35) Cylindrical micelles have also been formed from block copolymers with amorphous polyferrocenylsilane blocks. See: (a) Wang, X.; Winnik, M. A.; Manners, I. *Macromolecules* **2005**, *38*, 1928. (b) Korczagin, I.; Hempenius, M. A.; Fokkink, R. G.; Cohen-Stuart, M. A.; Al-Hussein, M.; Bomans, P. H. H.; Frederik, P. M.; Vancso, G. J. *Macromolecules* **2006**, *39*, 2306.
(36) Massey, J. A.; Winnik, M. A.; Manners, I.; Chan, V. Z. H.; Ostermann, J. M.; Enchelmaier, R.; Spatz, J. P.; Möller, M. *J. Am. Chem. Soc.* **2001**, *123*, 3147−3148.
(37) Cao, L.; Massey, J. A.; Winnik, M. A.; Manners, I.; Riethmuller, S.; Banhart, F.; Spatz, J. P.; Möller, M. *Adv. Funct. Mater.* **2003**, *13*, 271−276.
(38) Wang, X. S.; Arsenault, A.; Ozin, G. A.; Winnik, M. A.; Manners, I. *J. Am. Chem. Soc.* **2003**, *125*, 12686−12687.
(39) Wang, X. S.; Winnik, M. A.; Manners, I. *Angew. Chem., Int. Ed.* **2004**, *43*, 3703−3707.

Table 1. DLS Studies on the Influence of Solvents on the Micellization Behavior of Un-Cross-Linked PI_{250}-*b*-PFS_{50} Micelles

sample entry	solvents (solubility parameter[a])	$R_h^{app}/\mu_2/\Gamma^{-2}$ [b]
1	hexane (14.9)	63 nm/0.09
2	decane (13.5)	50 nm/0.08
3	hexane:toluene (18.2) (9:1 by volume)	116 nm/0.11
4	hexane:THF (18.6) (9:1 by volume)	578 nm/0.08
5	hexane:THF (10:0.05 by volume)	88 nm/0.13
6	decane:THF (9:1 by volume)	122 nm/0.08

[a] Solubility parameter for PFS: 18.6 [43] [b] The R_h values measured at 90° do not reflect the real radius of the micelles as an equivalent spherical shape is assumed. TEM data (Figure 1) provide a direct measurement of the micellar length of the cylindrical micelles.

In this paper, as a follow up to our preliminary communication,[38] we report detailed studies on shell-cross-linked cylindrical micelles derived from PI-*b*-PFS. We describe the self-assembly behavior of PI-*b*-PFS, metal-catalyzed shell-cross-linking reactions, and investigations of the properties and applications of the resulting robust cross-linked PFS cylinders.

Results and Discussion

(1) Synthesis and Self-Assembly of PI_{250}-*b*-PFS_{50}. We synthesized PI-*b*-PFS using sequential anionic polymerization in THF at room temperature. The molecular weight and block ratio were determined using GPC and ^{1}H NMR. The block copolymers undergo self-assembly in hexane, a block-selective solvent for PI, leading to one-dimensional micellar structures. By adjusting the relative length of the PI block with respect to PFS segments, we could vary the morphology of the aggregates. In principle, when the blocks of PI are significantly smaller than those of PFS, the block copolymers tend to aggregate into tape-like lamellae. When the length of PI was designed to exceed that of the PFS segment, we observed exclusively cylinders.[33] In this work, we focused on the self-assembly to form cylinders from PI_{250}-*b*-PFS_{50} (the subscripts denote the number-averaged degree of polymerization of each block).

Although various types of self-assembled cylindrical micelles have been reported, controlling the length of these 1D objects is a difficult challenge.[41] We found that the apparent hydrodynamic radii (R_h^{app}) of the cylindrical PI_{250}-*b*-PFS_{50} aggregates varied greatly depending on solution conditions. As shown in Table 1, two micellar solutions were prepared in either hexane or decane (samples 1 and 2). Both solvents are selective for PI chains, leading to aggregates with PFS cores. As characterized by dynamic light scattering (DLS) at 90°, we found that the R_h^{app} of the micelles was significantly different, with values of 63 nm in hexane and 50 nm in decane. We speculated that this difference might be related to the quality of the solvent for the PFS core-forming block, since hexane has a solubility parameter ($\delta = 14.9$) closer to that of PFS ($\delta = 18.6$) than decane ($\delta = 13.5$) (see Table 1).[42] To test this idea, we made several samples of cylindrical micelles in a range of mixed solvents containing a small fraction of a common solvent, such as toluene or THF. DLS indicated that R_h^{app} increased for all of the micelles in mixed solvents (samples 3−6 in Table 1) and higher contents of a common solvent led to a larger R_h^{app} (samples 4−6 in Table 1), suggesting that the ability of the solvent to solvate the PFS core was related to the increase in size of the micelles. For the micelles in mixed solvents, the type of common solvent also influenced micellization behavior. As shown for samples 3 and 4 in Table 1, we prepared two micellar solutions containing either THF or toluene. Although these two solutions had an identical polymer concentration (1 mg/mL) and the same fraction of a common solvent (10% by volume), the micelles in the solution containing THF had R_h^{app} of 578 nm and were significantly larger than those in the solution containing toluene with R_h^{app} of 116 nm. In previous studies we showed that THF is a better solvent for PFS than toluene,[43] so the effect of a common solvent on micellization could again be attributed to the solvency for the PFS core-forming block ($\delta = 18.6$). All of our DLS studies indicated that the solvent quality for PFS is an important factor determining the length of the PI-*b*-PFS micelles.

The nature of the solvent also determined the kinetics of the micellization. In the absence of a common solvent, we found the R_h^{app} was constant once prepared in either hexane or decane, regardless of the micellization conditions. In one experiment, we incubated a PI_{250}-*b*-PFS_{50} solution in hexane at 60 °C overnight and found there was no change in R_h^{app} during this thermal treatment, suggesting the structure was fully frozen even at this elevated temperature. Unlike the micelles in pure hexane, when a common solvent was present during micellization the micelles usually grew slowly at room temperature before reaching a constant R_h^{app}. The evolution usually lasted a few days depending on solution conditions. For instance, the micelles in decane/THF (9/1 by volume) (sample 6 in Table 1) grew from 92 nm to a constant R_h^{app} of 122 nm over 12 h. When hexane was used to replace decane (sample 4 in Table 1), the light scattering intensity for the sample was initially very weak after the sample was prepared but kept rising steadily and eventually reached a constant value after 4 days, corresponding to extremely large aggregates with R_h^{app} of 578 nm. A comparison of these two experiments suggested the growth of PI-*b*-PFS micelles might be related to the mobility of the PFS chains, since PFS would be expected to be more flexible in hexane/THF than in decane/THF.

Concurrent with the DLS experiments, we analyzed the cylindrical micelles using transmission electron microscopy (TEM) (Figure 1). Figure 1a and b displays images of the PI_{250}-*b*-PFS_{50} micelles that were self-assembled in pure decane and hexane, respectively. Figure 1c−e represent cylinders formed in mixed solvents. In all cases, we observed cylinders with very similar widths but lengths that varied from several hundreds of nanometers to several tens of micrometers. The variation in length measured from the images is fully consistent with the difference of R_h^{app} observed in Table 1.[44] In other words, the length of the cylinders was approximately proportional to the R_h^{app} measured by DLS. The combination of DLS and TEM studies indicated that solution conditions could be varied to obtain PI-*b*-PFS cylindrical micelles with various lengths in a controlled way.

Eisenberg and co-workers also reported the effect of a common solvent on the length of PS-*b*-PAA (PS, polystyrene,

(40) Wang, X. S.; Wang, H.; Coombs, N.; Winnik, M. A.; Manners, I. *J. Am. Chem. Soc.* **2005**, *127*, 8924−8925.
(41) Choucair, A.; Eisenberg, A. *Eur. Phys. J. E* **2003**, *10*, 37−44.
(42) For comparison, PI has a solubility parameter of 17.0.
(43) Kulbaba, K.; MacLachlan, M. J.; Evans, C. E. B.; Manners, I. *Macromol. Chem. Phys.* **2001**, *202*, 1768−1775.
(44) All data in Table 1 are apparent R_h values measured at 90°. The data do not reflect the real lengths and radii of the micelles. TEM provide direct measurement of the micellar lengths.

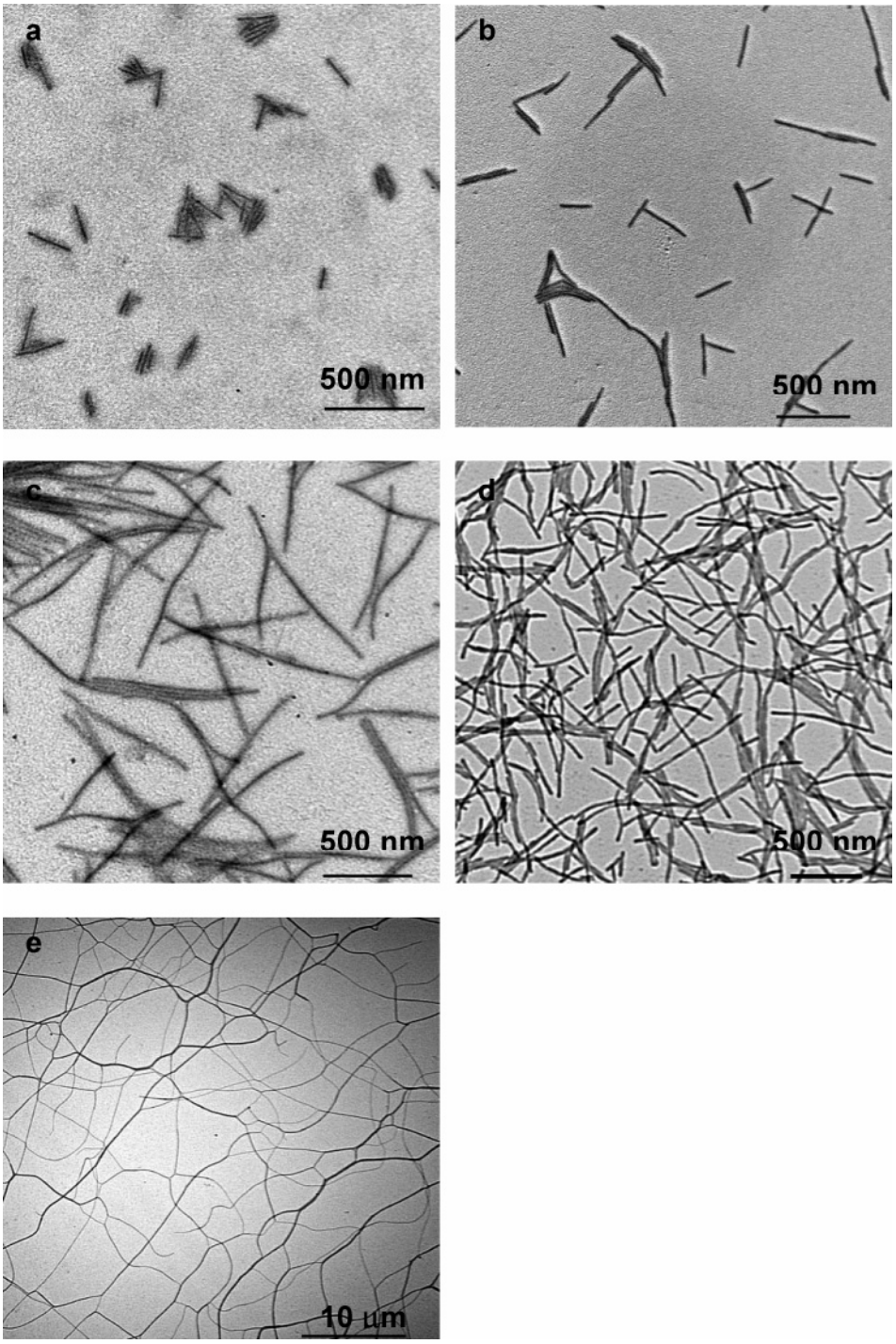

Figure 1. TEM images for cylindrical micelles self-assembled from PI_{250}-*b*-PFS_{50} in (a) decane, (b) hexane, (c) hexane/toluene (9:1 by volume), (d) hexane/THF (10:0.05 by volume), and (e) hexane/THF (9:1 by volume).

PAA, poly(acrylic acid)) cylindrical micelles in water.[41] They found the aggregates could be shortened by addition of a common solvent, THF, to the system. This result was explained by an interfacial energy term: the improvement in the solubility of the PS core-forming blocks by adding THF decreases the surface tension of the micelles, leading to a larger interfacial area by decreasing micellar size and simultaneously increasing the number of micelles. In contrast, we observed an opposite phenomenon: longer cylinders were formed in the solution containing a common solvent. We postulate that this might be ascribed to the crystallization behavior of PFS, which is a dominating factor governing the self-assembly.[34,35] It appears that growth of PFS crystalline cores is favored upon swelling of the PFS chains,[45] and this crystallization force seems to be strong enough to overwhelm other factors during the formation of micelles.

(2) Cross-Linking of Cylindrical PI_{250}-*b*-PFS_{50} Micelles Using Pt(0)-Catalyzed Hydrosilylation. Taking advantage of the peripheral vinyl groups of the PI corona chains, we attempted a number of reactions[46] to cross-link the shell of the micelles

(45) In a separate experiment, we found that the crystallinity of PFS thin films can be improved by annealing under an atmosphere of a good solvent.

Scheme 1

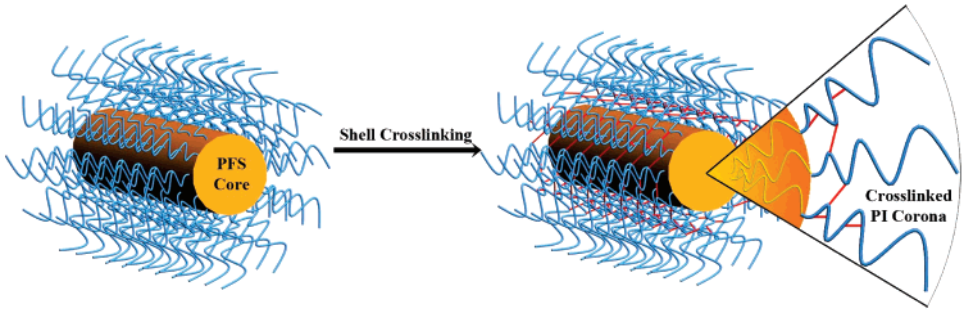

and found that Pt(0)-catalyzed hydrosilylation was the best choice for this purpose. We carried out a model reaction using vinyldimethylsiloxy-terminated polydimethylsiloxane with triethoxysilane in the presence of Pt(0) catalyst in hexane at room temperature. ^{1}H NMR analysis of the product indicated that all vinyl groups were consumed, suggesting that hydrosilylation could be used for shell-cross-linking with the PI_{250}-*b*-PFS_{50} micelles remaining intact.

Following micellization, we therefore induced a Pt(0)-catalyzed hydrosilylation cross-linking reaction using 1,1,3,3-tetramethyl disiloxane as a cross-linker at room temperature (Scheme 1). During the reaction, we withdrew aliquots from the reaction mixtures and transferred the micelles in hexane to a common solvent such as toluene or THF for DLS measurements. The R_h^{app} value in the common solvent deduced from DLS analysis enabled us to monitor the reactions. For unreacted samples, the aggregates disassembled in the common solvent into unimers with R_h^{app} of several nanometers. On the other hand, once the cross-linking reaction occurred we observed R_h^{app} values much larger than those of individual unimers. It is useful to have a term that describes the changes in dimensions that occur when a cross-linked structure is transferred from a selective solvent to a common solvent. We found it is convenient to compare the apparent hydrodynamic radii of the shell-cross-linked micelles in PI-selective hexane to the values in the common solvent THF measured at a 90° scattering angle. We refer to the ratio as the degree of swelling (DOS): DOS = R_h^{app}(THF)/R_h^{app}(hexane).

The hydrosilylation reaction is a relatively slow process, which usually last several days depending on the concentration of the cross-linkers and catalysts. As shown in the Table 2, when a 0.15 molar ratio of cross-linker relative to the total number of vinyl groups on the PI chains was added, the original micellar structures were not fully cross-linked until the reaction had been carried out for 14 days. The degree of cross-linking of the micelles was limited by the small amount of cross-linker used in the reaction. Upon transfer to THF solution, the micelles swelled substantially with a DOS of 1.52 and the value of the micelles' polydispersity index (μ_2/Γ^2) broadened to 0.23 relative to 0.10 in hexane. This broadening in μ_2/Γ^2 could be caused by certain degree of structural rupture upon swelling due to incomplete cross-linking.

(46) We explored several methods for the cross-linking reactions and encountered setbacks for most reactions. For example, free radical reactions led to insurmountable intermicellar cross-linking. Vulcanization of PI corona using S_2Cl_2 avoided intermicellar cross-linking but caused oxidation of the PFS core of the micelles. Attempted olefin metathesis using a commercially available Ru catalyst was also unsuccessful, presumably due to the poor solubility of the catalyst in hexanes.

Table 2. DLS Analysis of Shell-Cross-Linked PI_{250}-*b*-PFS_{50} Micelles[a]

no.	cross-linker/vinyl groups	reaction media	catalyst[d]/ polymer (mol %)	time (days)	DOS (μ_2/Γ^2 in hexane/THF)
1	0.15	hexane	0.1	8	partial cross-linking[e]
				14	1.52 (0.12/0.23)
2	0.40	hexane	0.1	4	1.58 (0.13/0.22)
				7	1.16 (0.11/0.12)
3	1	hexane	0.1	4	1.18 (0.09/0.10)
4	1	hexane	0.2	2	1.19 (0.10/0.09)
5	2	hexane	0.2	2	<1.05 (0.11/0.10)
6[b]	1	hexane/THF	0.1	4	1.26 (0.13/0.11)
7[c]	2	hexane/toluene	0.2	2	<1.03 (0.11/0.12)

[a] PI_{250}-*b*-PFS_{50} in hexane solution (10 mg/10 mL); the R_h of the aggregates was 63 nm. [b] PI_{250}-*b*-PFS_{50}/hexane/THF (10 mg/10 mL/0.05 mL). [c] PI_{250}-*b*-PFS_{50}/hexane/toluene (10 mg/10 mL/1 mL). [d] Karstedt's catalyst (2.5% Pt(0) complex in xylene). [e] R_h was 24 nm for the cross-linked aggregates in THF.

As we added more cross-linker or catalyst (samples 2−4 in Table 2), the reaction time decreased to a few days, leading to cross-linked structures with relatively low DOS. When the cross-linkers are less than or comparable to the total number of vinyl groups, a moderate DOS was obtained in the range from 1.16 to 1.20. Further increasing the amount of cross-linker to 2 equiv relative to the total vinyl groups, we produced cross-linked micelles with almost no swellability upon transfer to THF (samples 5 and 7).[47]

The cross-linking reaction was also applied to the micelles in hexane containing a common solvent. As previously noted, a small fraction of a common solvent swelling the PFS segments caused a slow growth of the micelles. Using the hydrosilylation reaction, we were able to covalently freeze the aggregates (samples 6 and 7 in Table 2). For example, we prepared micelles in a hexane/toluene (9:1 v:v) mixture and carried out the reaction 2 h later. At this point, the R_h^{app} for the un-cross-linked sample was 103 nm. Upon cross-linking, the R_h^{app} in the same solvent was 97 nm with a DOS of 1.03 (sample 7 in Table 1), and this value of R_h^{app} stayed constant. In contrast, the un-cross-linked aliquot kept growing with time and reached 116 nm after 5 days.

The purpose of the cross-linking reaction was to preserve the shape of PFS micelles under various conditions. TEM

(47) As mentioned by a reviewer, for a difunctional cross-linker, the presence of an excess of cross-linker should decrease the extent of cross-linking due to the stoichiometric imbalance (assuming equal functional group reactivity, the degree of cross-linking should drop by a factor of 4 when 2 equiv of the cross-linker are used). However, we observed an *increase* in the degree of cross-linking when an excess of cross-linker is used. We presume that this is a result of the unequal reactivity of the two ends of the cross-linker: once one end reacts, the second end reacts much faster due to its close proximity to the Pt catalyst and the neighboring vinyl groups in the micelle.

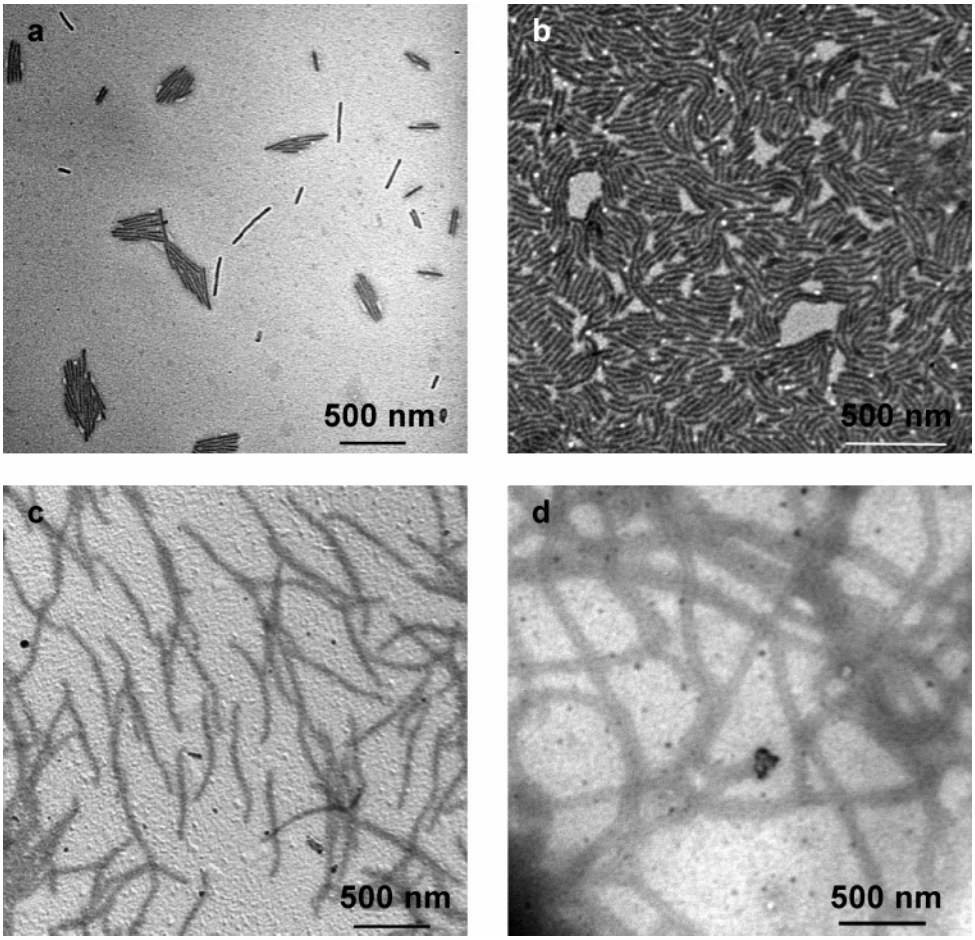

Figure 2. TEM images for shell-cross-linked PI_{250}-*b*-PFS_{50} micelles dried from (a) hexane or (b−d) THF solution. The cross-linked structures were synthesized in (a, b) hexane, (c) hexane/toluene (9/1 by volume), or (d) hexane/THF (9/1 by volume).

experiments provided a means to directly compare the morphologies of cross-linked micelles before and after the original solvents were replaced by a common solvent. The images of the aggregates in either hexane or THF are compared in Figure 2a and b. As shown in Figure 2a, the morphology of the micelles after cross-linking in hexane was virtually identical to that of the un-cross-linked counterpart (see Figure 1b), suggesting that hydrosilylation had no destructive effect on the aggregates. The desired shape retention upon cross-linking was confirmed by the image of the sample dried from THF solution (see Figure 2b). As shown in Figure 2b, one can see that the shape of cylinders is perfectly preserved but that they have become relatively flexible compared to the apparently rigid cylinders in Figure 2a. This slight change in the cylinders' appearance could be attributed to the dissolution of PFS crystallites upon transferring from hexane, a poor solvent, to THF, a good solvent for PFS block.[38,39] The successful cross-linking reactions in the systems containing a small fraction of common solvent allowed us to achieve much longer structures. We performed two cross-linking reactions in a solvent mixture composed of hexane with 10% by volume of toluene or THF. After reaction, the solvents were replaced by THF followed by TEM analysis of the samples prepared from THF solution of cross-linked micelles. The images are shown in Figure 2c and d. The cylinders in both of these samples are clearly longer than those cross-linked in pure hexane (Figure 2b), suggesting that the Pt(0)-catalyzed shell cross-linking reaction works with not only short cylinders but also longer aggregates. Therefore, through hydrosilylation of PI-*b*-PFS micelles it is possible to produce colloidal stable organometallic cylinders with various aspect ratios.

TEM experiments also provided an opportunity to visually appreciate the swelling and shrinking of shell-cross-linked micelles depending on the solution conditions as the micelles appear to pin to the substrate surface during solvent evaporation for sample preparation. A sample was prepared from a THF solution of cross-linked aggregates with a DOS of 1.52 (see sample 1 in Table 2) and examined using TEM. As shown in the image (Figure 3a), the width of the cross-linked aggregates was calculated to be ca. 55 nm, which is twice the original width for the micelles in hexane. In addition, one can discern that the swollen micelles do not seem as uniform as those in hexane (Figure 1a), suggesting incomplete cross-linking as inferred by the broadening of PDI in the DLS analysis (see sample 1 in Table 2). To this THF solution we added hexane dropwise until the volume ratio of hexane:THF reached 2:1 and then prepared a sample for TEM analysis. As illustrated in Figure 3b, the width calculated from the image is 27 nm, very close to that of original aggregates in hexane (25 nm), indicating a substantial contraction of the swollen micelles. For samples with a moderate DOS (ca. 1.20), the swelling behavior was not obvious in TEM experiments. A possible reason could be the errors associated with the shrinkage of the swollen aggregates during evaporation of THF that occurs as a result of TEM sample preparation under vacuum.[48]

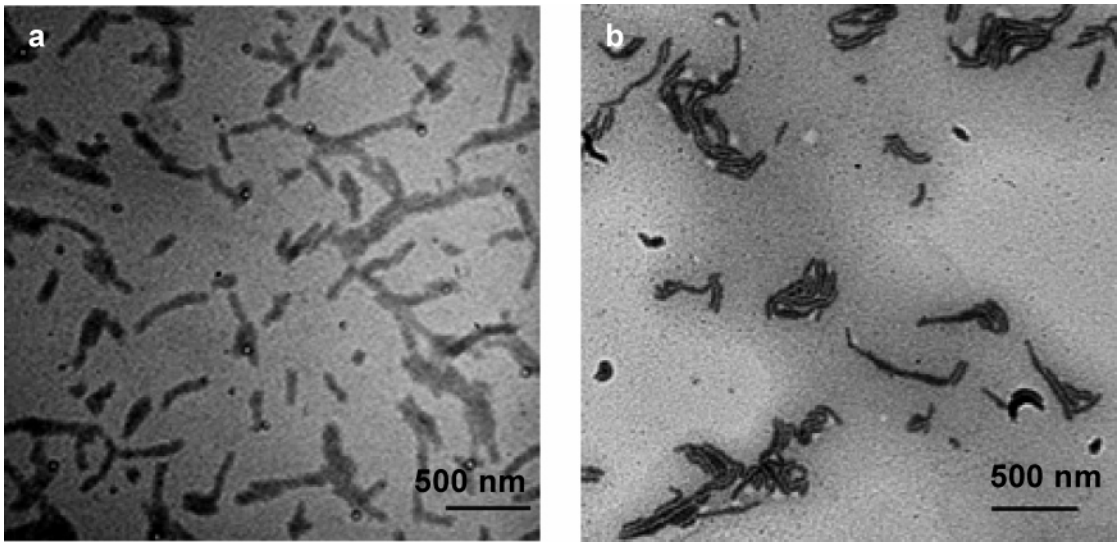

Figure 3. TEM images for (a) PI_{250}-*b*-PFS_{50} shell-cross-linked micelles dried from a solution in THF with a DOS of 1.52 and (b) the corresponding contracted micelles dried from hexane/THF solution (2/1 by volume).

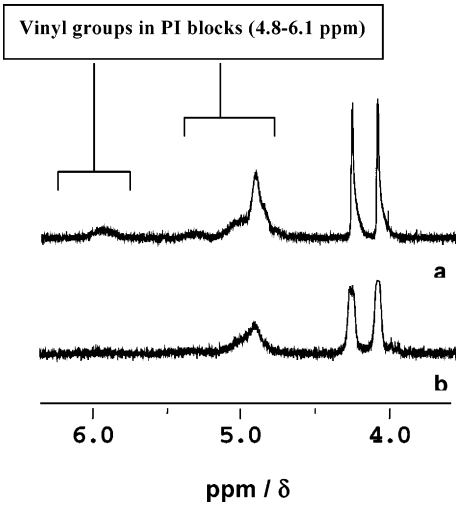

Figure 4. ^{1}H NMR (300 MHz) spectra in C_6D_6 for (a) PI_{250}-*b*-PFS_{50} and (b) the corresponding moderately shell-cross-linked micelles (DOS = 1.18).

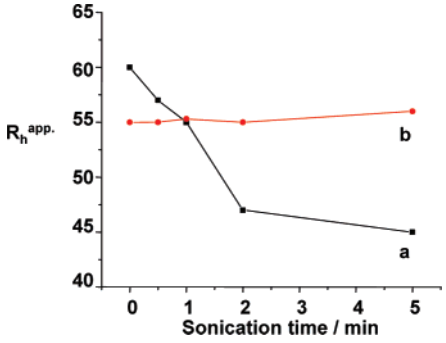

Figure 5. Apparent hydrodynamic radii of (a) PI_{250}-*b*-PFS_{50} un-cross-linked micelles and (b) cross-linked micelles measured at a scattering angle of 90° as a function of sonication time.

Table 3. Effect of Sonication on Apparent Hydrodynamic Radii of PI_{250}-*b*-PFS_{50} Shell-Cross-Linked Micelles Measured at a Scattering Angle of 90° in Various Solvents

PI_{250}-*b*-PFS_{50} aggregates	cross-linked micelles in hexane	nanogel in THF	nanogel in toluene
before sonication	54	63	53
sonication for 20 min	54	63	53
ΔR_h^{app}	0	0	0

The progress of the hydrosilylation cross-linking reaction was verified by ^{1}H NMR analysis of cross-linked micelles in C_6D_6, also a common solvent for both blocks. For the sample with a DOS of 1.03, the signals for the PFS and PI blocks were extremely broad and barely detectable by ^{1}H NMR due to the highly cross-linked network structure with only the CH_3-Si resonance being clearly defined. In the case of a relatively low degree of cross-linking (DOS = 1.18), the micelles are swellable and the mobility of the chains enabled us to detect the signals. As shown in Figure 4, the integration ratio of the resonances due to the double bonds (at 4.8−6.1 ppm) and those for the ferrocene units (at 4.1−4.4 ppm) was estimated and compared before and after shell cross-linking. On the basis of this comparison, ca. 36% of the double bonds were consumed.

(3) Properties and Patterning of the Shell-Cross-Linked PI_{250}-*b*-PFS_{50} Micelles. *(i) Mechanical Stability.* Self-assembled cylindrical PI_{250}-*b*-PFS_{50} micelles not only dissociate in common solvents but are also mechanically fragile as shown by ultrasonic experiments. We exposed the un-cross-linked micelles to ultrasound produced by a normal 40 W ultrasonic cleaning bath and monitored their R_h^{app} as a function of sonication time. As shown in Figure 5a, R_h^{app} decreased immediately upon sonication and leveled off after 2 min, suggesting poor structural integrity consistent with weak supramolecular interactions within the self-assembled structures. From previous studies, the crystallization and solvophobicity of PFS are the major forces holding the aggregates together, and these forces seem insufficient to resist ultrasound. Shell-cross-linking reactions introduced covalent bonds in the corona region, providing a strong intramicellar binding force in addition to the weak interactions within the cores of the micelles. As a result, unlike the sonication experiments on un-cross-linked micelles, the R_h^{app} for shell-cross-linked aggregates remained constant (see Figure 5b) during

(48) Apparently the micelles pin to the substrate surface while solvent evaporation occurs for the TEM measurement, enabling the swelling behavior to be examined. It is likely nevertheless that some size contraction occurs under these conditions.

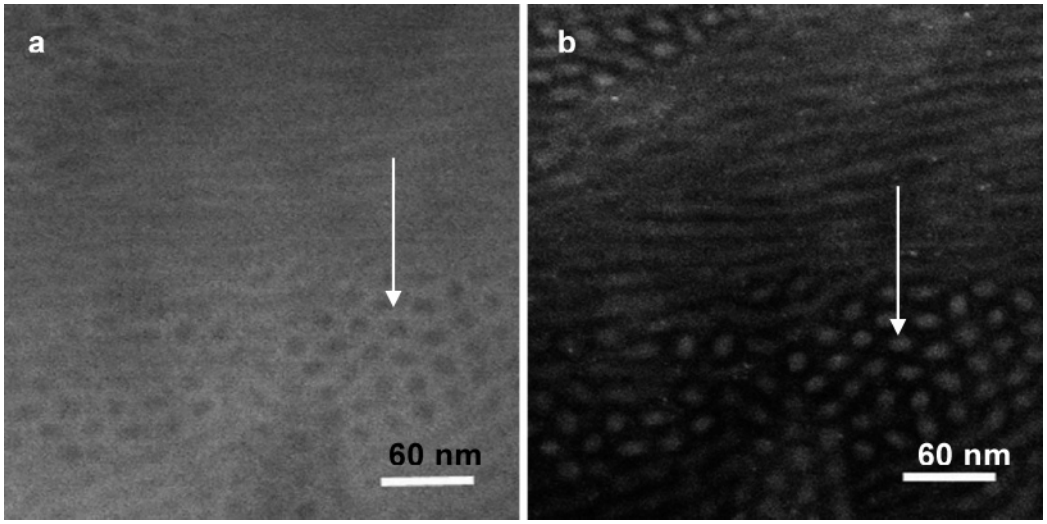

Figure 6. (a) Bright field and (b) dark field TEM images for cross-sections (indicated by arrows) of PI_{250}-*b*-PFS_{50} shell-cross-linked cylindrical micelles. The TEM sample was microtomed from a solid film dried from a hexane solution.

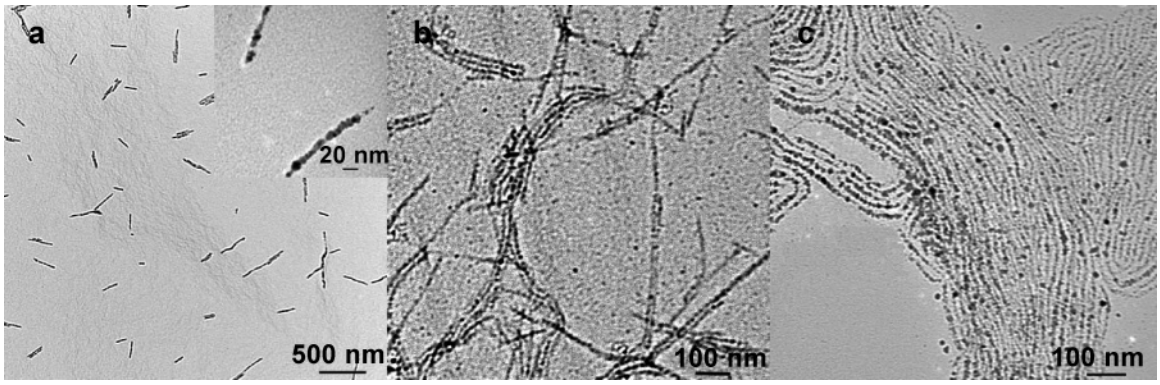

Figure 7. TEM images for ceramics generated through the pyrolysis at 600 °C of PI_{250}-*b*-PFS_{50} shell-cross-linked micelle precursors with various lengths. The precursors were cross-linked in and dried from (a) hexane, 1.00 DOS, (b) hexane/toluene, 1.16 DOS, and (c) hexane/THF, 1.26 DOS.

the course of sonication, making clear the dramatic improvement in stability of the assemblies imparted through shell cross-linking.

In a common solvent such as either THF or toluene, the core of PFS was dissolved but the shape of the cross-linked micelles was preserved by the covalent coronal bonds (see Figure 2). We can refer to these structures as a kind of cylindrical nanogel. We exposed PFS nanogels in either THF or toluene to ultrasound for 20 min and found, similar to the case of the aggregates in hexane, that there is no discernible reduction in R_h (Table 3). Apparently, these nanogels are as stable as the cross-linked micelles in hexane, even though the weak interactions in the core region are absent. As anticipated, covalent bonds indeed provide the major contribution to the improved mechanical stability of the shell-cross-linked PI-*b*-PFS micelles.

(ii) Cross-Sectional Analysis of the Micelles by TEM. As noted above, in the past we provided evidence that indicates that the cores of PFS cylindrical micelles such as those reported here are semicrystalline.[34] One unresolved question concerns the shape for the cross-section of the semicrystalline core. The answer to this question may help to shed some light on the PFS chain folding and the orientation of the crystallites. In previous studies, we observed that the width of PI-*b*-PFS micelles is larger than their height in AFM measurements.[37] This observation seemed to suggest that the core of the micelles might have a rectangular structure. However, the possible tip-related artifacts inherent to AFM imaging made it impossible to settle this question. We therefore attempted to directly view the shape of the cross-sections by microtoming solid samples of cross-linked PI_{250}-*b*-PFS_{50} micelles. This approach was hampered due to the possible deformation of original micellar structures upon transferring from discrete micelles to a monolithic bulk sample. Shell-cross-linked structures are therefore highly desirable as this could prevent PFS cores from fusing together and would ensure shape retention upon evaporation of solvent during sample preparation for microtoming. In addition, as a result of the disappearance of vinyl groups on PI chains consumed by hydrosilylation, the solid sample is quite rigid compared to that from the un-cross-linked block polymer, which favors successful microtoming.

The slices microtomed from the cross-linked micelles were examined by TEM. Representative images are illustrated in Figure 6. Both the bright field (Figure 6a) and dark field (Figure 6b) images indicate that the cross-section is a round shape with a diameter of ca. 15 nm, which is very similar to a head-on view of nanocylinders of semicrystalline poly(ethylene oxide) (PEO) confined within glassy polystyrene domains in the bulk state.[49] From this observation we can likely rule out a lamellar shape for the PFS cores. Further detailed

(49) Huang, P.; Zhu, L.; Cheng, S. Z. D.; Ge, Q.; Quirk, R. P.; Thomas, E. L.; Lotz, B.; Hsiao, B. S.; Liu, L.; Yeh, F. *Macromolecules* **2001**, *34*, 6649−6657.

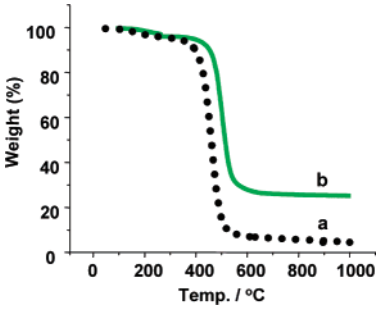

Figure 8. TGA traces obtained at a temperature ramp of 1 °C/min for PI_{250}-*b*-PFS_{50} solid samples dried from (a) un-cross-linked micelles and (b) shell-cross-linked micelles with DOS of 1.00.

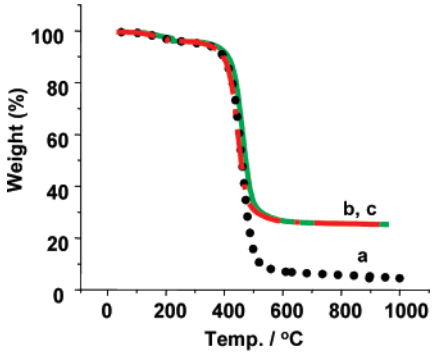

Figure 9. TGA traces obtained at a temperature ramp of (a) 10, (b) 1, and (c) 10 °C/min but incubated at 200 °C for 10 min for PI_{250}-*b*-PFS_{50} solid samples dried from cross-linked micelles.

characterization on the solid shell-cross-linked micelle samples may allow us to understand the details of the PFS crystalline structure.[49]

(iii) Nanoceramic Fabrication. The presence of metallic elements in polymer structures can introduce additional functionality.[29] For example, pyrolysis of PFS homopolymers yields magnetic ceramics without shape retention of the original precursors. The ceramics contain iron nanoclusters dispersed within an amorphous C/SiC matrix.[50] Use of cross-linked PFS materials as precursors led to high ceramic yields as well as excellent shape retention.[51,52] In an attempt to create nanoscale magnetic ceramic objects, we attempted to pyrolyze un-cross-linked PI_{250}-*b*-PFS_{50} cylindrical micelles at 600 °C. Unfortunately, TEM showed that the original shape of micelles was totally destroyed, presumably due to the lack of a cross-linked structure. In striking contrast, shell-cross-linked PI_{250}-*b*-PFS_{50} cylinders with various lengths produced ceramics with excellent shape retention upon heating to 600 °C under N_2 with a temperature ramp of 1 °C/min. As shown in Figure 7, the ceramics consist of Fe nanoclusters with diameters of ca. 10−15 nm, and their lengths correspond approximately to those of the precursor micelles. The nanoclusters could be closely packed (Figure 7a) or arranged as beads on a string (Figure 7b and c). In Figure 7c one can even observe some particles larger than 20 nm. Because the DOS of the original precursors was 1.00, 1.16, and 1.26 for the ceramics in Figure 7a,b, and c, respectively, it appears likely that the proximity and size of Fe clusters is a function of the degree of cross-linking. These results indicate that shell cross-linking plays an essential role in shape retention and permits the formation of ceramic replicas.[52]

To understand the effect of shell cross-linking on ceramic formation, we performed thermogravimetric analysis (TGA) experiments of both cross-linked and un-cross-linked micelles under the same conditions used for pyrolysis. As shown in Figure 8, the cross-linked precursors generated ceramics having ca. 30% of their original mass. If we assume that all of the ceramic residue is derived from the PFS component, the ceramic yield based on PFS is ca. 83%. This yield is much higher than that for PFS homopolymers but only slightly less than that for highly cross-linked PFS bulk materials.[50−52] In a control experiment with un-cross-linked micelles, only 3% of the original weight was retained under the same conditions of thermal treatment. Clearly the high ceramic yield is due to cross-linking and the major reason for shape retention during pyrolysis is likely to be that the loss of potentially volatile PFS-derived fragmentation products through the corona is hindered.[50]

We further examined the effect of the thermal treatment on ceramic yields by performing TGA experiments with varied temperature ramps. All precursors used in the experiments were shell-cross-linked. As shown in Figure 9a, when we increased the temperature ramp up to 10 °C/min, the ceramic yield dropped to less than 5%. Interestingly, under the same ramp but with a temperature plateau at 200 °C for 10 min (Figure 9b), the thermal weight loss profile was almost identical to that for the same cross-linked sample treated with a continuous temperature ramp of 1 °C/min (Figure 9c), both conditions generating high ceramic yield. These experiments suggest that incubating the precursors at a relatively high temperature or a slow ramp is required for high mass retention. However, it is important to note that cross-linking is a prerequisite for high ceramic yield because un-cross-linked micelles, upon thermal treatment at either 1 or 10 °C/min with a plateau at 200 °C for 10 min, always produced a low ceramic yield (less than 5%). The incubation period presumably allows some additional network forming chemical reactions to occur within the sample, such as radical coupling, which would favor mass retention during the pyrolysis.

(iv) Microfluidic Alignment. Alignment of one-dimensional nano-objects on flat substrates is an essential step for their detailed physical characterization and potential nanodevice fabrication. Several methods have been developed for this purpose, including microfluidic channel-assisted alignment. When a solution of shell-cross-linked PI-*b*-PFS cylinders was placed at the edge of an array of microchannels, it spontaneously filled the channels through capillary forces, provided that surface interactions were favorable. Upon evaporation of solvent in the channels, the cylinders tend to be concentrated and align along the edge of the microchannels.[36,37,53,54]

Cross-linked micelles are colloidally stable and can be manipulated in various solvents, which proved optimal for the microfluidic-patterning method. Our initial experiment with cross-linked micelles in hexane indicated inefficient patterning because hexane swells PDMS stamps, thus deforming the

(50) (a) Tang, B.-Z.; Petersen, R.; Foucher, D. A.; Lough, A.; Coombs, N.; Sodhi, R.; Manners, I. *J. Chem. Soc., Chem. Commun.* **1993**, 523−525. (b) Petersen, R.; Foucher, D. A.; Tang, B.-Z.; Lough, A.; Raju, N. P.; Greedan, J. E.; Manners, I. *Chem. Mater*. **1995**, *7*, 2045−2053.
(51) MacLachlan, M. J.; Ginzburg, M.; Coombs, N.; Coyle, T. W.; Raju, N. P.; Greedan, J. E.; Ozin, G. A.; Manners, I. *Science* **2000**, *287*, 1460−1463.
(52) Ginzburg, M.; MacLachlan, M. J.; Yang, S. M.; Coombs, N.; Coyle, T. W.; Raju, N. P.; Greedan, J. E.; Herber, R. H.; Ozin, G. A.; Manners, I. *J. Am. Chem. Soc.* **2002**, *124*, 2625−2639.
(53) Hahn, J.; Webber, S. E. *Langmuir* **2004**, *20*, 1489−1494.
(54) Yang, P.; Kim, F. *Chem. Phys. Chem.* **2002**, *3*, 503−506.

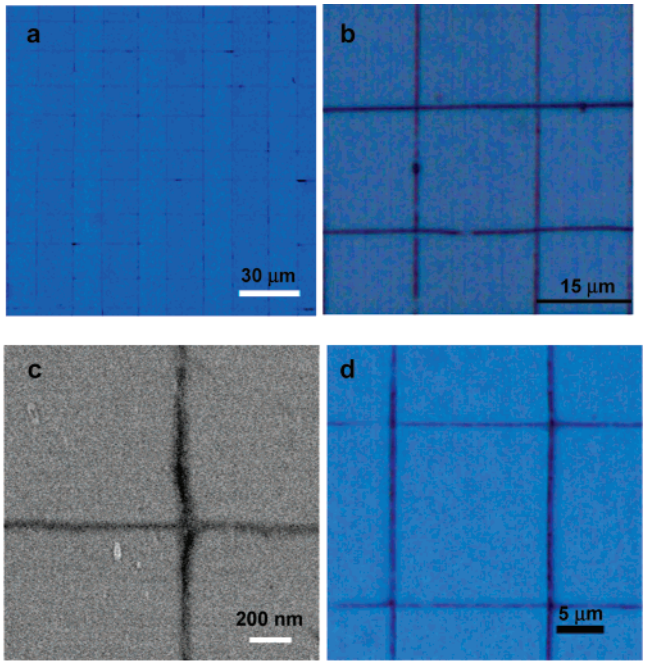

Figure 10. (a) Low-magnification optical image, (b) high-magnification optical image, and (c) SEM image of microfluidically aligned cross-patterned cross-linked PI_{250}-*b*-PFS_{50} micelles, and (d) optical image of the corresponding ceramic replicas.

microchannels. We alleviated this problem by replacing hydrophobic PDMS stamps with stamps made of the more polar polyurethane (PU) elastomer. As shown in Figure 10a and b, we were able to show by optical microscopy that micelles could be aligned into a crossed array through a two-step experiment. Scanning electron microscopy (SEM) experiments allowed us to view the lines at high resolution. As indicated in Figure 10c, one can see a cross of aligned lines that are obviously thicker than single micelles, suggesting they are micelle bundles. As shell-cross-linked PFS aggregates can be used as ceramic precursors, we attempted to pyrolyze the aligned micelles. The ceramics were characterized by optical microscopy, and a typical image is displayed in Figure 10d. As shown in the figure, we obtained patterned ceramic lines. The continuous lines of the ceramic are of interest to create rows of carbon nanotubes by catalysis[30] and as magnetic nanostructures for device applications.

Summary

Through the self-assembly of PI_{250}-*b*-PFS_{50} in hexane or hexane mixed with a small fraction of a common solvent, we are able to obtain organometallic cylindrical micelles with various lengths. The presence of a common solvent leads to longer aggregates, presumably due to the enhanced growth of PFS crystalline cores. By comparing the effect of two common solvents, the solution containing THF generates 1D fibers much longer than those obtained in the solution with the same fraction of toluene. As THF can swell PFS gels better than toluene, we infer that the degree of swelling of the PFS core favors growth of the aggregates.

Taking advantage of vinyl groups pendent to the PI corona chains, we successfully performed Pt(0)-catalyzed shell-cross-linking reactions on PI_{250}-*b*-PFS_{50} cylindrical micelles, leading to stable organometallic 1D nanostructures with adjustable length. As a result of shell cross-linking, many previously unsuccessful attempts to characterize and utilize PFS micelles have become possible. (a) Using a sonication experiment, we could show that the cross-linked materials are much more stable than un-cross-linked analogs. (b) The cross-linked structure prevented potential deformation of the cylindrical shape when the micelles were dried from solution. Therefore, from TEM experiments on microtomed solid samples of the cross-linked micelles we have been able to show that the shape of the cross-section of the PI_{250}-*b*-PFS_{50} cylindrical aggregates is circular. (c) Shell-cross-linked micelles were used as precursors to generate 1D magnetic ceramic replicas. TGA analysis suggested that both cross-linking and the incubation of the precursors at an intermediate temperature (prior to massive mass loss) are important for high ceramic yields and shape retention. (d) By imbibing a solution of shell-cross-linked micelles in hexane into microchannels formed from a polyurethane elastomeric microstamp, we were able to pattern the cross-linked micelles on flat substrates through microfluidic alignment. These results indicate that these and related shell-cross-linked organometallic cylinders are easily processed, dimensionally stable nanostructures with a variety of promising applications.

Acknowledgment. M.A.W. and I.M. thank the Emerging Materials Knowledge program of Materials and Manufacturing Ontario for funding. I.M. thanks the European Union for a Marie Curie Chair and the Royal Society of Chemistry for a Wolfson Research Merit Award. G.A.O. is a Government of Canada Research Chair in Polymer and Materials Chemistry. We thank one of three reviewers for their comment on the effect of the amount of cross-linkers on the cross-linking reaction (see ref 47).

Supporting Information Available: Experimental section. This material is available free of charge via the Internet at http://pubs.acs.org.

JA068730F